Biomedical and environmental applications of SR-TXRF and SR-TXRF-XANES

Christina Streli
Atominstitut
streli@ati.ac.at

ICTP-IAEA School on Novel Experimental Methodologies for Synchrotron Radiation Applications in Nano-science and Environmental Monitoring

November 2014

Total Reflection XRS

E D X R F

Standard XRF | Micro XRF μ-XRF | Total Reflection XRF TXRF | Absorption Spectroscopy in fluorescence mode (XAS

Advantages

- background reduction
- double excitation of sample
- small distance sample ⇔ detector (~1mm) ⇨ large solid angle

⇨ Low detection limits

- low sample mass require
- angle dependence of fluorescenc signal

⇨ information about type of sample (bulk, particle, film, implantation)

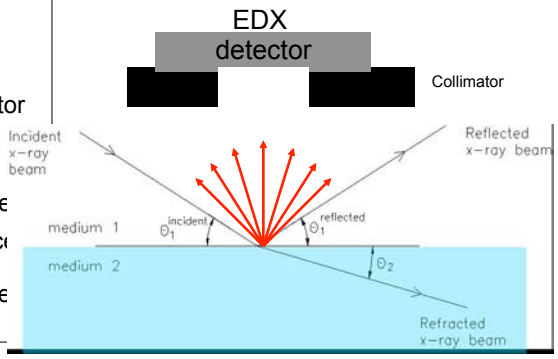

Total (external) reflection of X-Rays

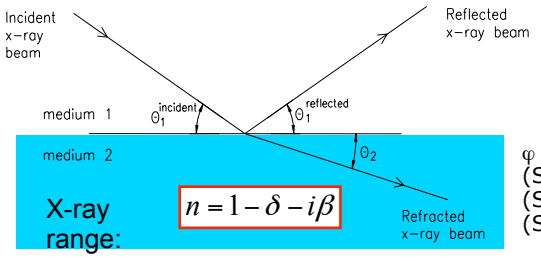

X-ray range: $n = 1 - \delta - i\beta$

$$\Phi_{crit} \approx \sqrt{2 \cdot \delta} \approx \frac{20.7}{E} \cdot \sqrt{\rho}$$

ϕ_{crit} [mrad], E [keV], ρ [g·cm^{-3}]

φ critical
(Si, 17.5 keV) ≈ 0.1° ≈ 1.75 mrad
(Si, 500 eV) ≈ 3.7° ≈ 64.6 mrad
(Si,12.2 keV) ≈ 0.15° ≈ 2.6 mrad

$\delta \sim 10^{-6}$ … dispersion:
$\beta \sim 10^{-8}$ … absorption:

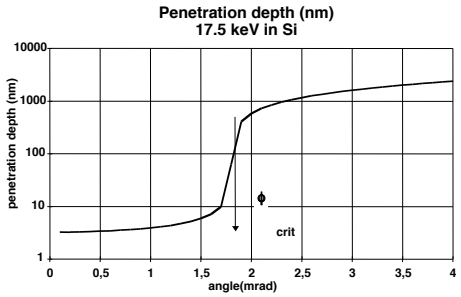

Advantages of TXRF

- **small sample amounts required (ng, some µl)**
- **detection limits in the pg range with X-ray tube excitation**
- **detection limits in the fg range with Synchrotron radiation excitation**
- **Simple quantification (thin film approximation) by adding internal standard**
- **angle dependence of fluorescence signal : particle – film - implantation**

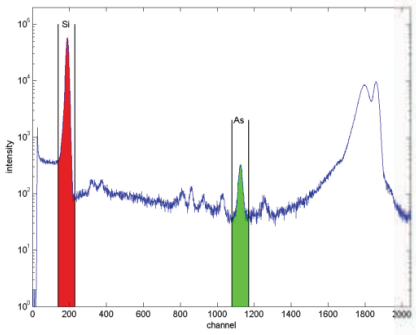

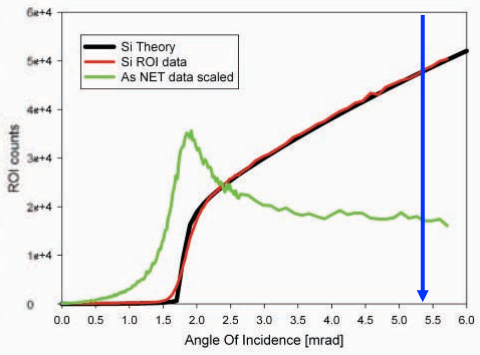

Comparison of water standard reference sample

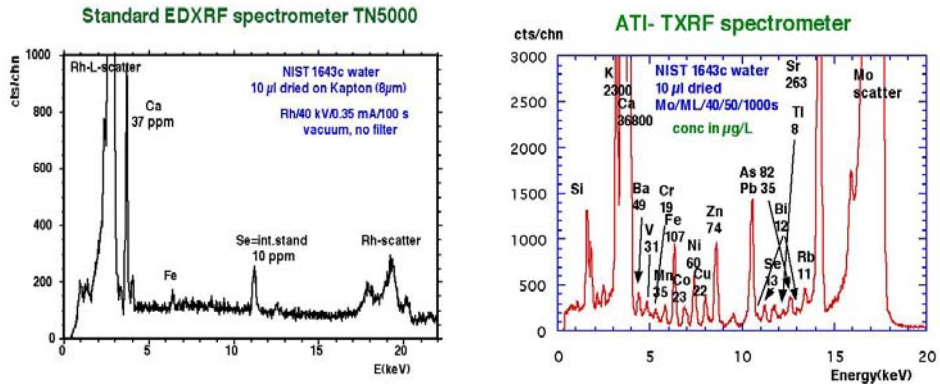

Quantification in TXRF

Quantification in TXRF

Calibration curves relative to internal standard for each element:
Determination of relative sensitivities

Interpolation for not measured elements:

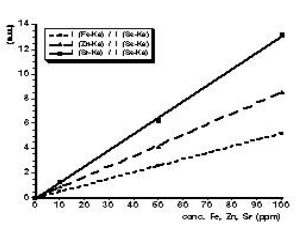

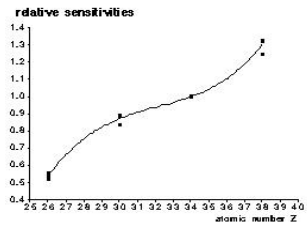

Determination of concentration of element i relative to internal standard:

$$c^i = \frac{I^i}{I^s} \cdot \frac{1}{S^i_{rel}} \cdot c^s$$

C.Streli 2002

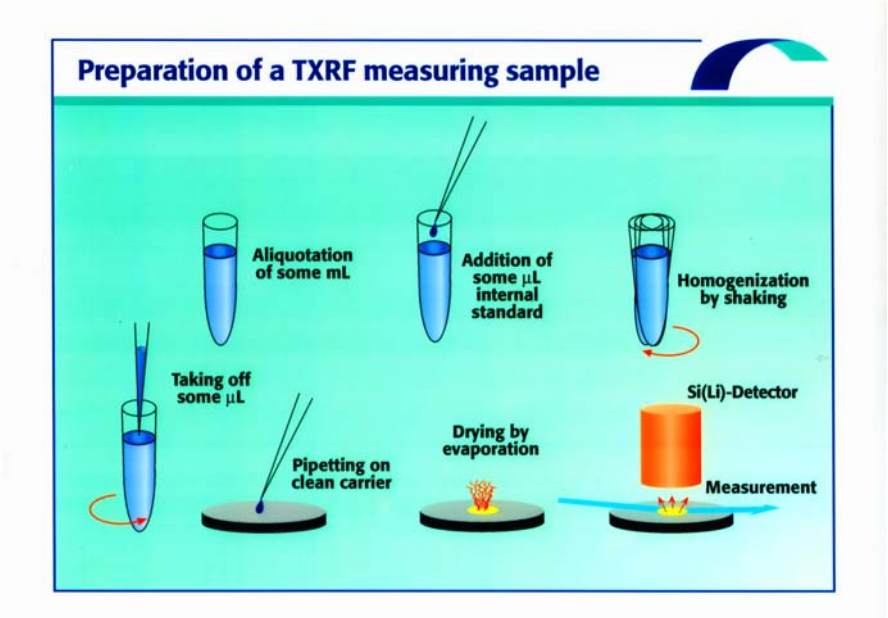

Applications of TXRF

Environment:

water:	rain, river, sea, drinking water, waste water.
air:	aerosols, airborne particles, dust, fly ash.
soil:	sediments, sewage sludge.
plant material:	algae, hay, leaves, lichen, moss, needles roots, wood.
foodstuff:	fish, flour, fruits, crab, mussel, mushrooms nuts, vegetables, wine, tea.
various:	coal, peat.

Medicine / Biology / Pharmacology:

body fluids:	blood, serum, urine, amniotic fluid.
tissue:	hair, kidney, liver, lung, nails, stomach, colon.
various:	enzymes, polysaccharides, glucose, proteins, cosmetics, bio-films.

Industrial/Technical applications:

surface analysis:	Si-wafer surfaces, GaAs-wafer surfaces
implanted ions	depth and profile variations
thin films	single layers, multilayers
oil:	crude oil, fuel oil, grease.
chemicals:	acids, bases, salts, solvents.
fusion/fission research:	transmutational elements in Al + Cu, Iodine in water

Mineralogy:

ores, rocks, minerals, rare earth elements.

Fine Arts / Archeological / Forensic:

pigments, paintings, varnish.
bronzes, pottery, jewelry.
textile fibers, glass, cognac, dollar bills, gunshot residue, drugs, tapes, sperm, finger prints.

Why Synchrotron Radiation?

- High Intensity
- High collimation vertical to the orbital plane (little angular divergence)
- Continuos energy distribution ⇨ monochromators can be used over a wide range of energies
- Photons are highly polarized in the orbital plane ⇨ significant background reduction in EDXRF

Detection Limits in the fg range for medium Z Elements

$$LLD = \frac{3}{S} \cdot \sqrt{\frac{I_B}{t}}$$

Influence of radiation source upon S and I_B:

- Intensity (larger S and I_B)
- Spectral distribution (monochromatic excitation ⇨ smaller I_B)
- Linear polarization (smaller I_B)

Seite 9

Experimental Setup @ HASYLAB beamline L

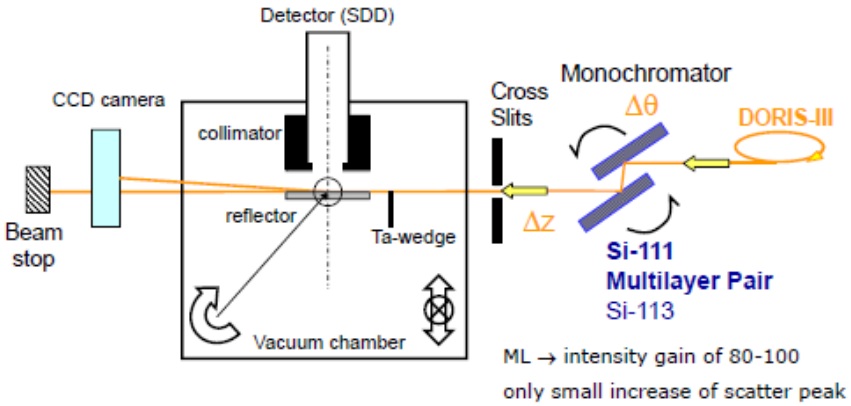

ML → intensity gain of 80-100

only small increase of scatter peak

sample changer 8 stages

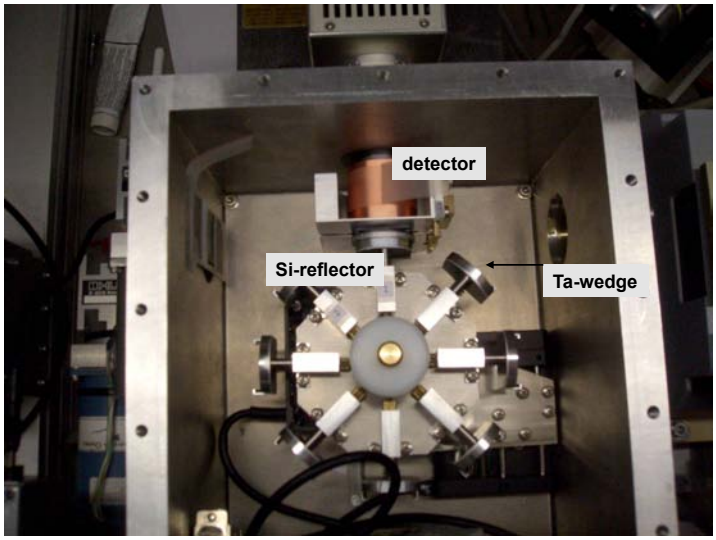

SR-TXRF measurements HASYLAB, Beamline L (bending magnet)

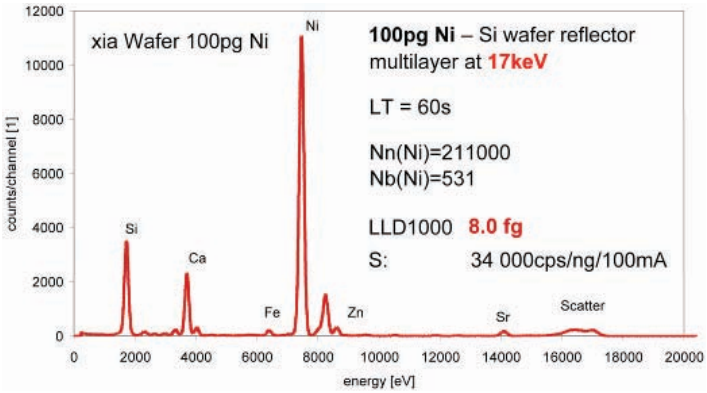

SR-TXRF:
8 fg detection limits in 1000s at 17keV
assuming an inspected area of 1cm² this value corresponds to 8E7 atoms/cm²

Example: The X-ray Absorption Fine Structure (XAFS) of an Fe-foil

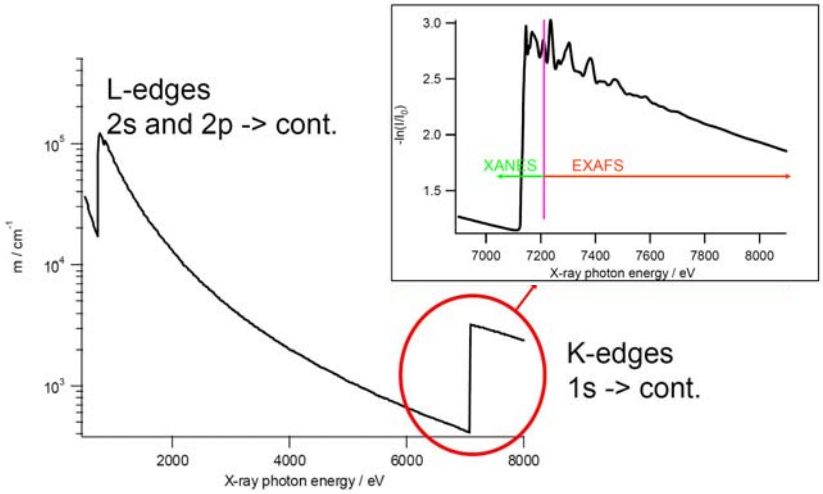

XANES: **X**-Ray **A**bsorption **N**ear **E**dge **S**tructure, ends 50-100 eV above the edge
EXAFS: **E**xtended **X**-Ray **A**bsorption **F**ine **S**tructure, starts 50 - 100 eV above the edge

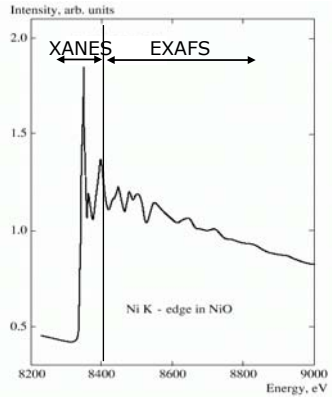

The x-ray absorption spectrum shows a fine structure if it is sampled with a high resolution.

absorption involves electronic transitions

fine structure affected by energy and density of electronic states and transition probabilities

influence of the environment: neighbouring atoms (EXAFS), bond type (XANES)

$$W_{if} = \frac{2\pi}{\hbar} \left| \langle \Psi_i | \hat{H}_I | \Psi_f \rangle \right|^2 \rho(E_f)$$

EXAFS XANES

XANES: **X**-Ray **A**bsorption **N**ear **E**dge **S**tructure, ends 50-100 eV above the edge
EXAFS: **E**xtended **X**-Ray **A**bsorption **F**ine **S**tructure, starts 50 - 100 eV above the edge

Introduction - The EXAFS Experiment

Variation of excitation energy

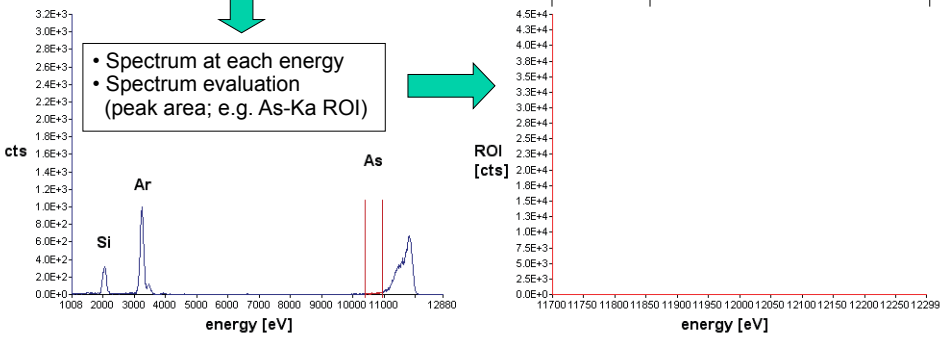

EXAFS XANES

$$W_{if} = \frac{2\pi}{\hbar} \left| \langle \Psi_i | \hat{H}_I | \Psi_f \rangle \right|^2 \rho(E_f)$$

EXAFS equation, Fingerprint method (XANES)

• XANES: bond type
• EXAFS: neighboring atoms

Application: analysis of aerosols: coop Dr. Fittschen

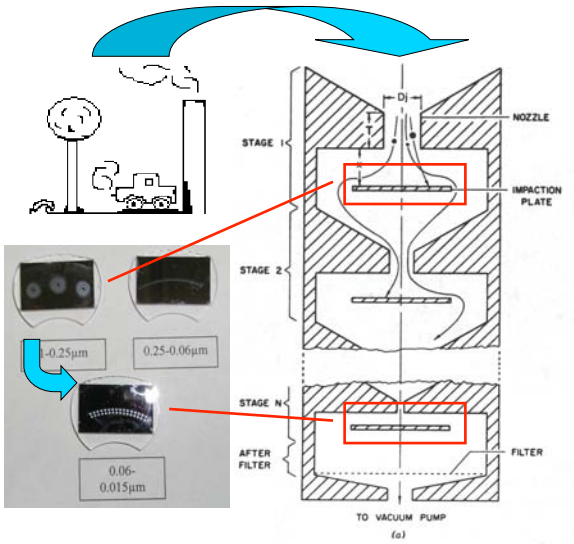

Motivation:

To understand the effect of aerosols on global climate a detailed understanding of sources, transport, fate and the physical and chemical properties of atmospheric particles necessary.

Aerosol particle sampling device, 12-stage, round nozzle **Berner low-pressure impactor** for particle sizes of 0.06-12 µm (aerodynamic particle size);

Quantification with picodroplets

Coop: U.Fittschen, J.Broekaert, Univ, Hamburg

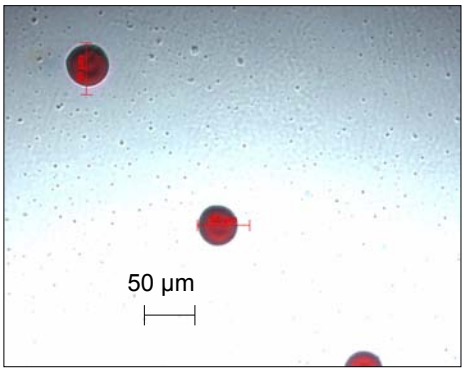

Light microscope image of ink pico-droplets printed by HP PSP 1000 printer (~ 5 pL) on a silicone coated quartz reflector

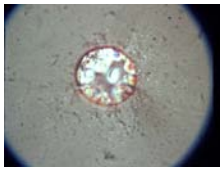

Droplet size 20 µm

Calibration curve

Coop: U.Fittschen, J.Broekaert, Univ, Hamburg

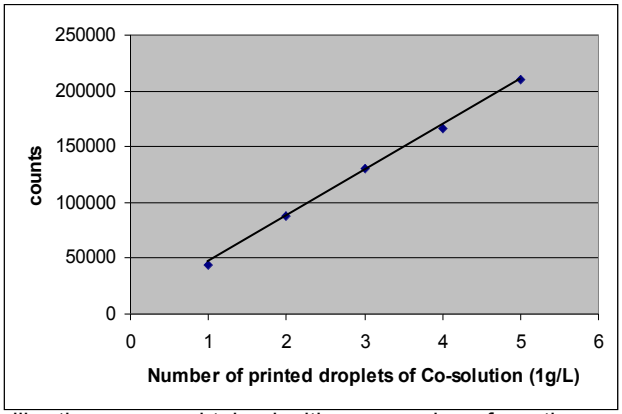

Calibration curves obtained with mean values from three series for: five times 1 droplet of a 1 g/L cobalt standard solution spotted successively with a HP 500C printer on a quartz reflector

SR-TXRFanalysis of aerosols

Advantages of SR-TXRF:

- only small sample mass required
- sampling time can be diminished
  ⇨ time resolved investigation of atmosph
- simple sample preparation
  (aerosols directly collected on reflectors)

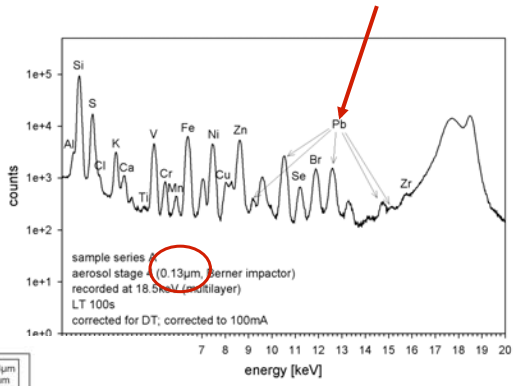

20 min sampling time !

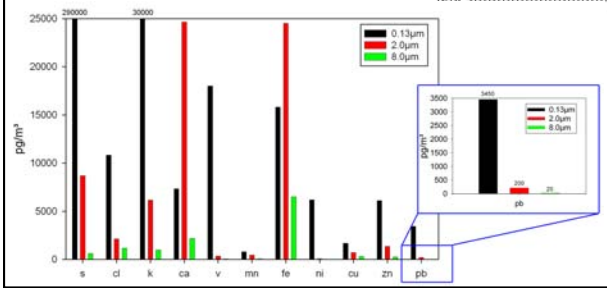

Pb high in very small particles < 130 nm!

TXRF- (& XANES) analysis of aerosols

Fe K-edge Aerosols

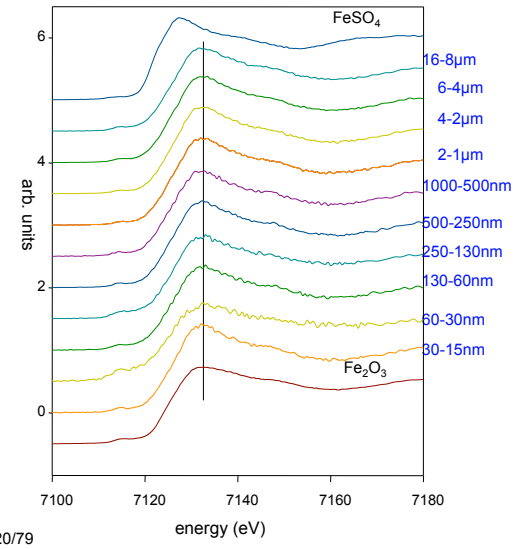

All stage showed Fe(III)!

Spectrochimica Acta Part B 63 (2008) 1489–1495

Contents lists available at ScienceDirect

Spectrochimica Acta Part B

journal homepage: www.elsevier.com/locate/sab

Characterization of atmospheric aerosols using Synchroton radiation total reflection X-ray fluorescence and Fe K-edge total reflection X-ray fluorescence-X-ray absorption near-edge structure☆

U.E.A. Fittschen [a,*], F. Meirer [b], C. Streli [b], P. Wobrauschek [b], J. Thiele [a], G. Falkenberg [c], G. Pepponi [d]

Trace element analysis and zinc speciation in size-fractionated aerosol samples using SR-TXRF and XANES

J. Osán,[1] V. Groma,[1] F. Meirer,[2] E. Börcsök,[1] S. Török,[1] C. Streli,[2] P. Wobrauschek[2] and G. Falkenberg[3]

[1]KFKI Atomic Energy Research Institute, P.O. Box 49, H-1525 Budapest, Hungary
[2]Atominstitut der österreichischen Universitäten, TU Wien, Vienna, Austria
[3]HASYLAB at DESY, Hamburg, Germany

Methods

- SR-TXRF for elemental analysis in minute amounts of samples in each size fraction
- Direct sampling on Si wafer reflectors to avoid contamination caused by sample pre-treatment
- Speciation information of heavy metals in minute amount of size-fractionated aerosol using TXRF-XANES
- Sampling with cascade impactor on polluted and background sites

Size fractioned aerosol sampling

- 7-stage May-type cascade impactor
- cut-off diameters: 16, 8, 4, 2, 1, 0.5, 0.25 μm for stages 1-7 at 20 lpm flow rate
- sampling 20-3200 l air depending on stages and aerosol concentration

The deposited aerosol particles form a 200-500 μm wide strip in the middle of the Si wafer of 20x20 mm^2

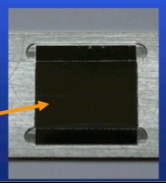

SR-TXRF(-XANES) measurements

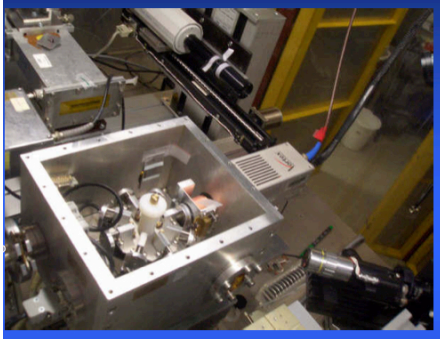

- new vacuum chamber [1] at HASYLAB beamline L
- automatic sample loader, easy sample change
- various sizes and shapes of samples can be measured

[1] *Streli C., Pepponi G., Wobrauschek P., Jokubonis C., Falkenberg G., Zaray G., 2005:. A new SR-TXRF vacuum chamber for ultra-trace analysis at HASYLAB, Beamline L. X-Ray Spectrom., 34, 451–455*

- SR beam dimensions 1.4 mm (vertical) x 0.2 mm (horizontal)
- SDD with 1.4 mm wide Mo slit collimator (sample geometry)
- **TXRF:** E_0=18.4 keV, ΔE/E=0.02 (multilayer monochromator) sample was scanned over a length of 6 mm in 6 steps, with beam perpendicular to the strip
- **TXRF-XANES:** Si(111) monochromator tuned around Zn-K edge (9659 eV), sample strip parallel to the beam

Standards

A. Resuspension of solid particles of known composition, sampling with the same equipment as used for ambient aerosols
→ Geometry and size distribution of standard samples is the same as for unknown samples at each impactor stage
ZnO standard for XANES

B. Nanoliter injector
$Zn(NO_3)_2$ standard for XANES (1-10 ng)
Single- and multielemental calibration standards for TXRF

C. Cr strip on Si wafers exactly on the same position as particles from the air sample – external standard for TXRF, prepared by MFA [2]

[2] *Watjen U., Bársony I., Dücső C., 2000: A Novel Micro-Structured Reference Material for Ion and X-Ray Microbeam Analysis, Mikrochim. Acta, 132, 521–525*

SR-TXRF detection limits

Element	Detection limit (pg/m3) Regular	Ultimate
S	451.3	164.0
Cl	282.8	102.7
Ca	70.2	25.5
Ti	48.7	17.7
Cr	23.4	8.5
Fe	12.4	4.5
Cu	4.5	1.6
Zn	3.5	1.3
Se	2.6	0.9
Br	2.4	0.9
Sr	3.4	1.2
Pb	5.3	1.9

Sample volume: 1000 l
Measurement time: 100 s
Ring current: 100 mA

Regular:
sample strip perpendicular to the beam
Ultimate:
sample strip parallel to the beam

V. Groma, J. Osán, S. Török, F. Meirer, C. Streli, P. Wobrauschek, G. Falkenberg Trace element analysis of airport related aerosols using SR-TXRF Időjárás 112 (2008) in press

TXRF results

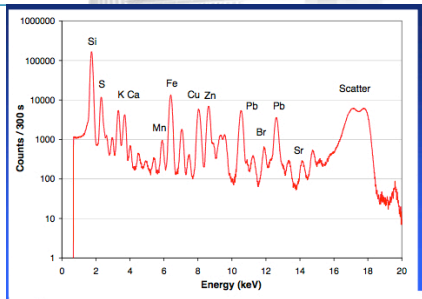

Typical SR-TXRF spectrum of an aerosol sample collected at Budapest, 0.5–1 μm size fraction

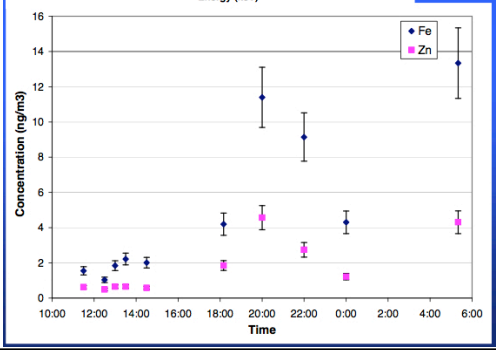

Temporal variation of Fe and Zn in the 0,5-1 μm aerosol fraction at Mátra (400 l air per sample)

Fe and Zn values show anticorrelation with the mixing layer height that was expected

Sampling sites

Aerosol samples were collected at various sites:
Inn-valley (Austria): urban (Innsbruck), highway, suburban (Imst),
Hungary: airport (Budapest), mountain
Background: (Mátra, H; Alps, A), Atlantic background station (Serreta, Acores, P)

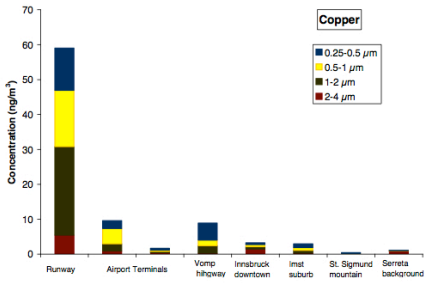

TXRF results

Heavy metals dominant in the submicrometer fractions → indicator of anthropogenic origin

Zn and Pb are related to areas where traffic sources dominate

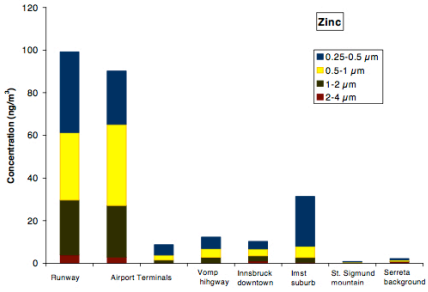

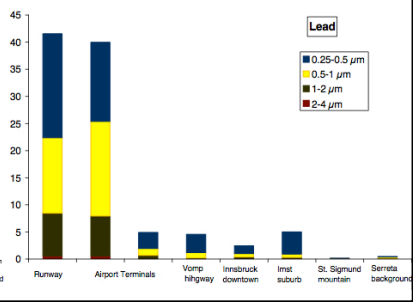

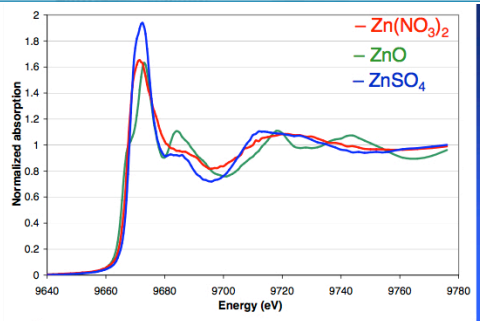

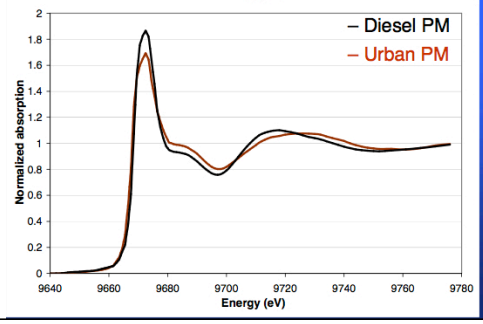

TXRF-XANES spectra

TXRF-XANES spectra of zinc nitrate, zinc oxide and yinc sulfate standards

Zn-K XANES spectra of NIST urban and diesel particulate matter standards [3]

→
diesel: more similar to $ZnSO_4$
urban: more similar to $Zn(NO_3)_2$

[3] *Huggins FE, Huffman GP, Robertson JD. Speciation of elements in NIST particulate matter SRMs 1648 and 1650, J Hazard Mater 2000, 74, 1-23*

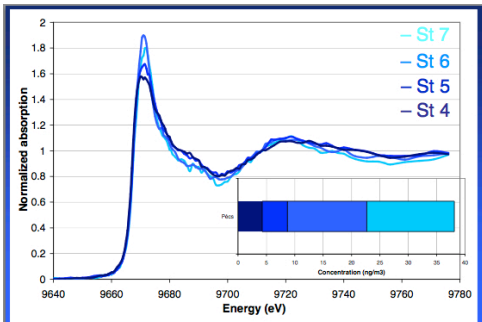

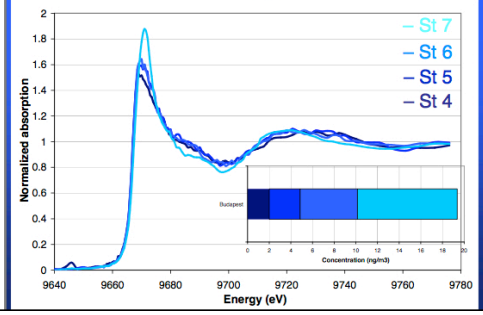

TXRF-XANES spectra

Pécs, city center

impactor stages 7,6,5,4 (0.25-0.5, 0.5-1, 1-2, 2-4 μm)

St 7,6,5: mixture of Zn sulfate and nitrate

St 4: mostly soil-originated Zn (e.g. $ZnCO_3$)

White line decrease with increasing particle diameter – not from self-absorption effect

Budapest, near bus garage

Zinc sulfate only in St 7

St 6,5,4: increased amount of soil-originated Zn (resuspension)

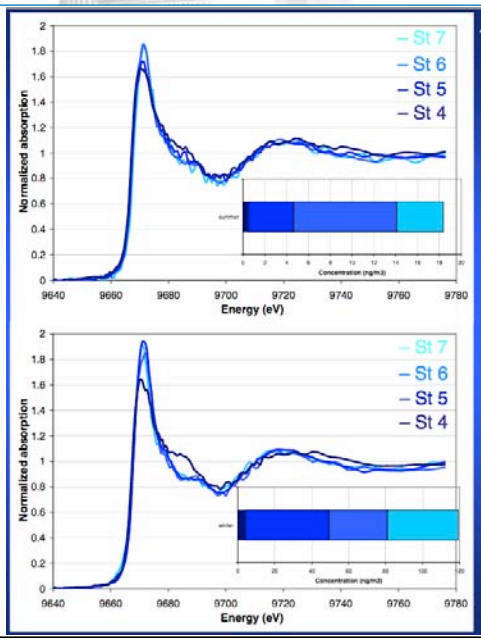

TXRF-XANES spectra

Budapest, summer

impactor stages 7,6,5,4 (0.25-0.5, 0.5-1, 1-2, 2-4 μm)

St 7,6,5: Zn connected mostly to nitrates

St 4: Zn nitrate and Zn carbonate

Budapest, winter

Zn concentrations 6 time higher than in summer – extremely low MLH

St 7,6,5: Zn connected mostly to sulfates

St 4: mostly soil-originated Zn ($ZnCO_3$)

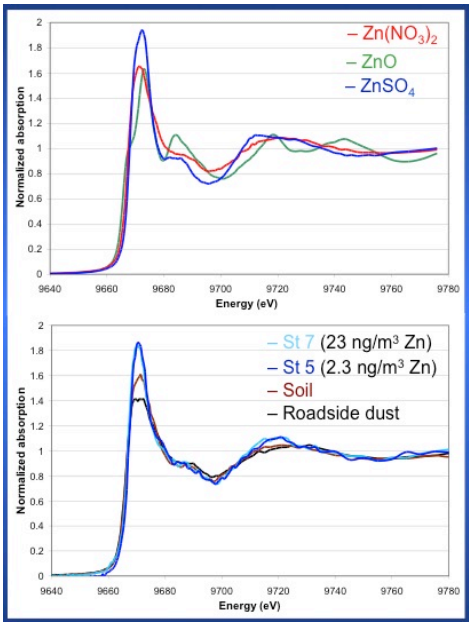

TXRF-XANES spectra

Zn-K absorption edge

TXRF-XANES spectra of zinc nitrate, zinc oxide and zinc sulfate standards

Imst, winter

St 7–5: Zn connected to nitrates and sulfates

Soil and roadside dust

Zn connected to carbonates and silicates

Conclusions

- Short time collection can allow one to study temporal variation of elemental concentrations in size-fractionated aerosol
- Detection limits in the pg/m^3 range can be reached for a 20-min sampling time
- Further potential
  1. Time resolved trace element analyses in havaria/emergency situation using portable TXRF
  2. Potential to use in industrial/traffic processes where the time scale of the event is similar to the typical sampling durations
- Information on Zn speciation using TXRF-XANES from air Zn concentrations as low as 100 pg/m^3
- Zn connected to sulfates and nitrates in submicron particles

Spectrochimica Acta Part B 65 (2010) 1008–1013

Contents lists available at ScienceDirect

Spectrochimica Acta Part B

journal homepage: www.elsevier.com/locate/sab

Speciation of copper and zinc in size-fractionated atmospheric particulate matter using total reflection mode X-ray absorption near-edge structure spectrometry

János Osán [a,*], Florian Meirer [b,c], Veronika Groma [a], Szabina Török [a], Dieter Ingerle [c], Christina Streli [c], Giancarlo Pepponi [b]

Speciation of arsenic in xylem of plants

Cooperation with Prof.Zaray and Dr. Mihucz, Eötvös Univ, Budapest

In the south-eastern part of Hungary arsenic is a known contaminant in groundwater which can reach concentrations up to 150 ng/mL.

The World Health Organisation (WHO) recommends an upper limit of 10 ng/mL for arsenic in drinking water.

Concerning plants arsenate acts as an analogue of phosphate, competing for the same uptake carriers in the root.

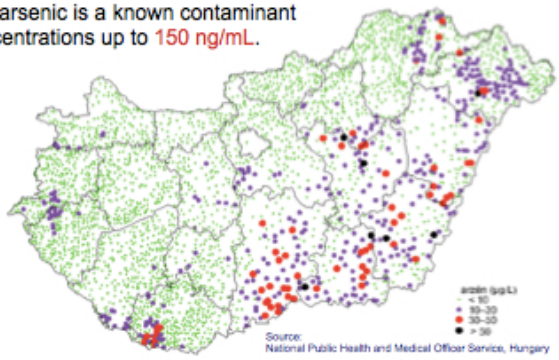

Plants have the capability to change the oxidation state of arsenic.

The toxicity of arsenic differs considerably dependent on the oxidation state and chemical form.

Speciation of arsenic in xylem of plants

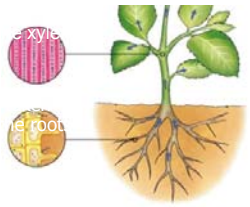

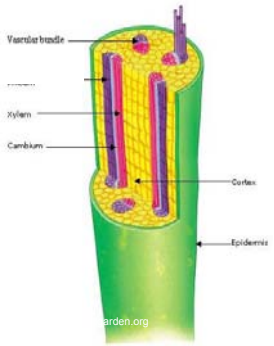

Motivation 1:
- understand how plants metabolise and transform As
- assess the health risk caused by As entering the food chain (different As species have different toxicity)

⇨ Speciation of arsenic (As[III] or As[V]) in xylem

Problem:
Previous investigation of the cucumber xylem saps with flow injection analysis (FIA) and HPLC-HRICP-MS revealed arsenic concentrations in the 30–50 ng/ml (ppb) range.
⇨ Concentrations too low for standard XAS setup

Motivation 2:
- investigate competitive capability of SR-TXRF-XANES analysis for this application (vs. HPLC-HRICP-MS)

Speciation of arsenic in xylem of plants

Coop: Eötvös Univ. Budapest, Prof. Zaray, Dr. Mihucz

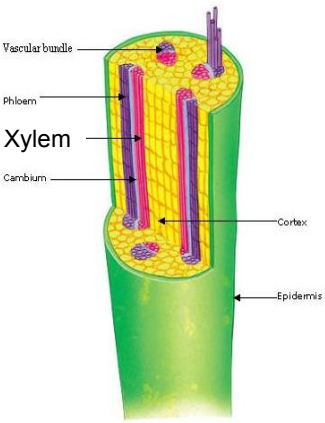

Source: www.fairchildgarden.org

Motivation:

Arsenic is contained in groundwater in Eastern Hungary (up to 2µmol). Speciation of As in xylem is important to:

- understand how plants metabolise and transform As
- assess the health risk caused by As entering the food chain (different As species have different toxicity; e.g. As(III) and As(V))

Experimental:

- At two leaf stage:
  transferred in solution with arsenic compounds and reduced phosphate concentration
- After 30 days from germination (17 d arsenic):
  - stem cut 2 mm above root neck
  - sap collected with micropipettes
    ⇨ for 1 hour into PE vials immersed in ice salt bath

Speciation of arsenic in xylem of plants

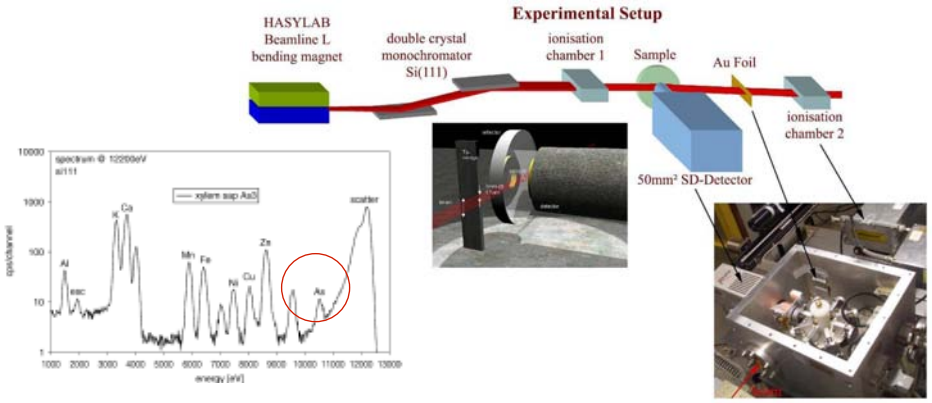

Advantages of XAS in TXRF geometry:

- TXRF offers good sensitivity for XANES speciation of traces (ppb range)
- only small sample volumes are required
- simple sample preparation (just pipetting some µl on reflectors)
  ⇨ prevents unwanted oxidation of sample during preparation

Speciation of arsenic in xylem of plants

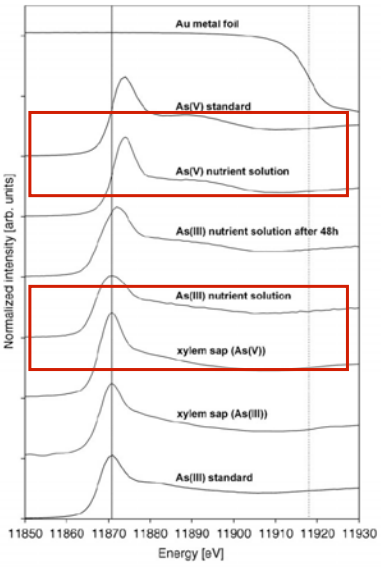

Results:

- Speciation of As was possible down to the 30ppb level
- As(III) in nutrient solutions oxidises easily to As(V)
- **Cucumber roots convert As(V) to As(III)**

- ***Best poster award*, Denver X-Ray Conference 2006**

- **F. Meirer et al., *Application of synchrotron-radiation-induced TXRF-XANES for arsenic speciation in cucumber (Cucumis sativus L.) xylem sap*, X-Ray Spectrometry 36 (2007) 408-412.**

Self absorption effect: F.Meirer

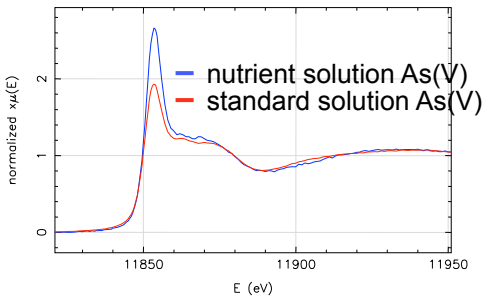

Example:
Speciation of arsenic in xylem of plants
standard solution As(V):
20µl of 10000ppb ⇨ 200ng
nutrient solution As(V):
20µl of 150ppb ⇨ 3ng

Self absorption seems to be responsible for the differences in the white line height

The Self-Absorption Effect

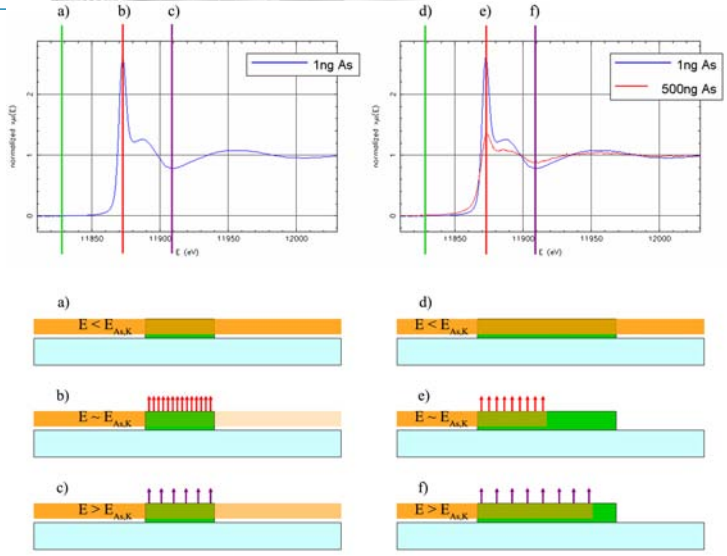

Self-absorption effects in TXRF-XANES

Investigation of the absorption effect depending on:

- the total mass deposited
- the three-dimensional shape of the sample
- the density of the element investigated

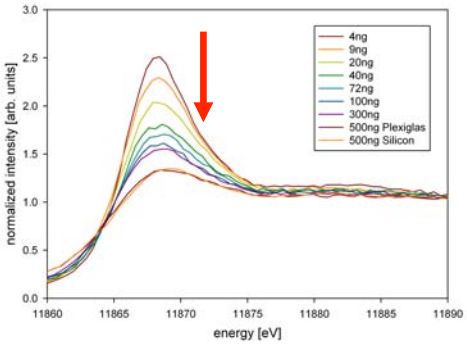

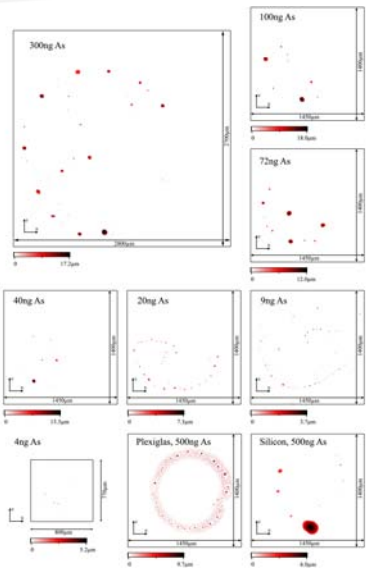

Self-absorption effects in TXRF-XANES

Investigation of the sample geometry by confocal microscopy:

Data of the 3 dimensional distribution of the droplet residue was used for a simple Monte Carlo simulation.

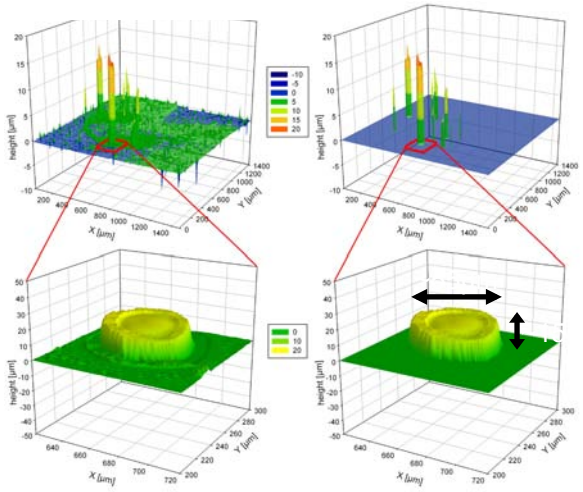

Zoom of the largest droplet of the 100ng As sample before (left) and after (right) threshold filtering.

Self-absorption effects in TXRF-XANES

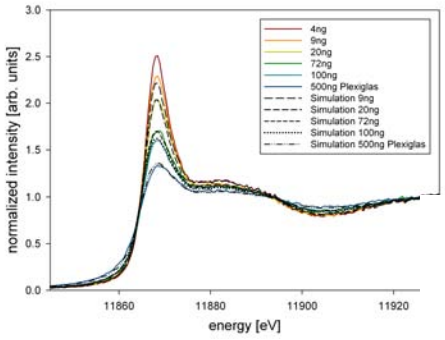

Monte Carlo simulation of the fluorescence considering sample geometry and density:

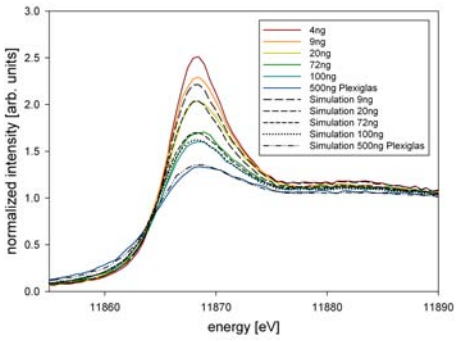

Results of simulations showed good agreement with measurements.

GE vs. TXRF geometry for XANES analysis

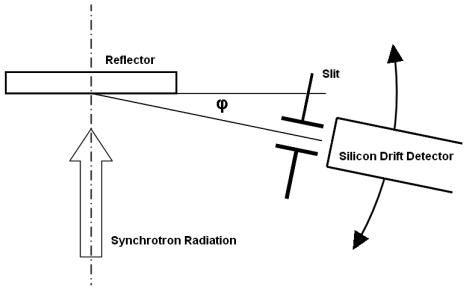

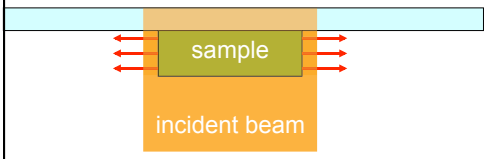

- GE experiment provides the same information as the GI experiment according to the optical reciprocity theorem
- Much smaller solid angle seen by the detector => lower DLs
- Incident beam can be focused (optics) => mapping capability

Assumption:

- No self-absorption effects in XAS experiments

Self-absorption effects in TXRF-XANES

Results:

- The damping of the oscillations of TXRF-XANES spectra are linearly correlated with the total mass of the samples
- Self absorption effects can be observed for sample amounts > 1 ng (for Arsenic)
- Sample density and geometry seems to play an important role (simulations considering these parameters showed good agreement with measurements)

Conclusions:

- EXAFS measurements for larger sample amounts will be very difficult
- Influences on sample parameters (e.g. sample preparation, carrier material, …) should be further investigated

Spectrochimica Acta Part B 63 (2008) 1496–1502

Contents lists available at ScienceDirect

Spectrochimica Acta Part B

journal homepage: www.elsevier.com/locate/sab

Parameter study of self-absorption effects in Total Reflection X-ray Fluorescence–X-ray Absorption Near Edge Structure analysis of arsenic☆

F. Meirer [a,*], G. Pepponi [b], C. Streli [a], P. Wobrauschek [a], P. Kregsamer [a], N. Zoeger [a], G. Falkenberg [c]

Conclusions

Advantages of XANES in TXRF geometry:

- TXRF offers good sensitivity for XANES speciation of traces
- only small sample volumes are required
- simple sample preparation (just pipetting some µl on reflectors)

⇨ prevents unwanted oxidation of sample during preparation

E D X R F

Standard XRF | Micro XRF μ-XRF | Total Reflection XRF TXRF | Absorption Spectroscopy in fluorescence mode (XA

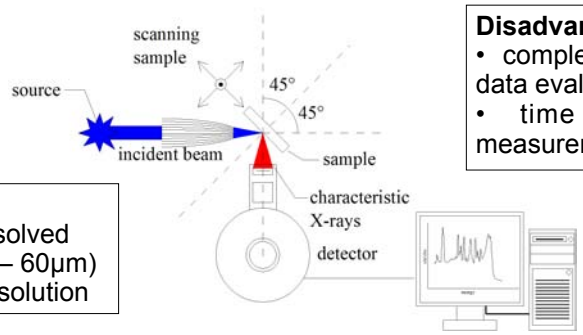

Disadvantages
- complex setup and data evaluation
- time consuming measurements

Advantages
- spatially resolved analysis (10 – 60μm)
- 2D & 3D resolution

Trace Element Distribution in Human Bone

B. Pemmer[1], A. Roschger[2], J. G. Hofstaetter[2,3], P. Wobrauschek[1], P. Roschger[2], K. Klaushofer[2], C. Streli[1]

[1] Atominstitut, Technische Universitaet Wien, Stationallee 2, 1020 Vienna, Austria
[2] Ludwig Boltzmann Institute of Osteology at the Hanusch Hospital of WGKK and AUVA Trauma Centre Meidling, 1st Med. Dept., Hanusch Hospital, 1140 Vienna, Austria
[3] Department of Orthopaedic Surgery, Vienna General Hospital, Med. Univ. of Vienna, Austria

MEDIZINISCHE UNIVERSITÄT WIEN

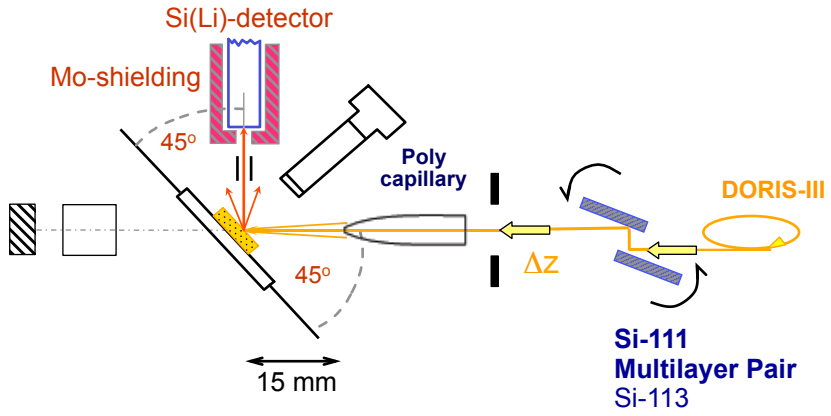

Focal size: 13-30 µm

Bone Structure

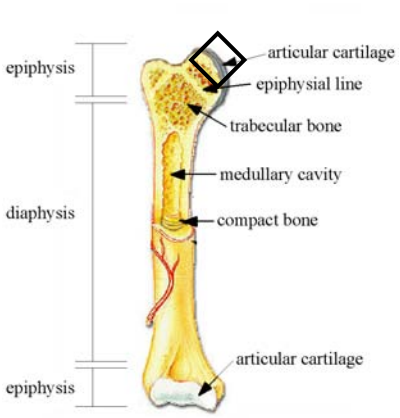

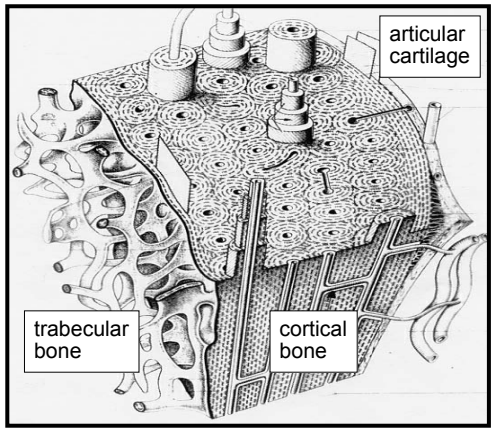

Bone Structure – Close Up 1

Backscattered Electron Image (BE), Patella

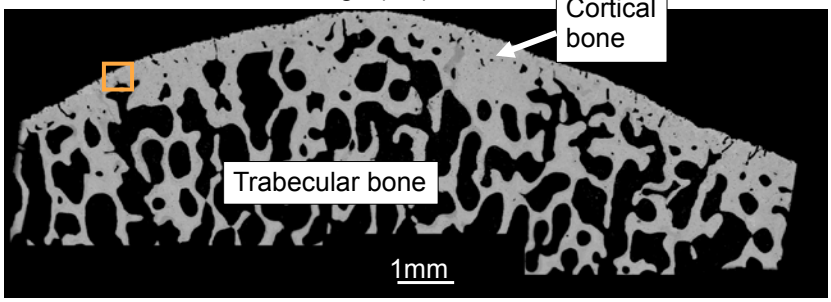

Bone Structure – Close Up 2

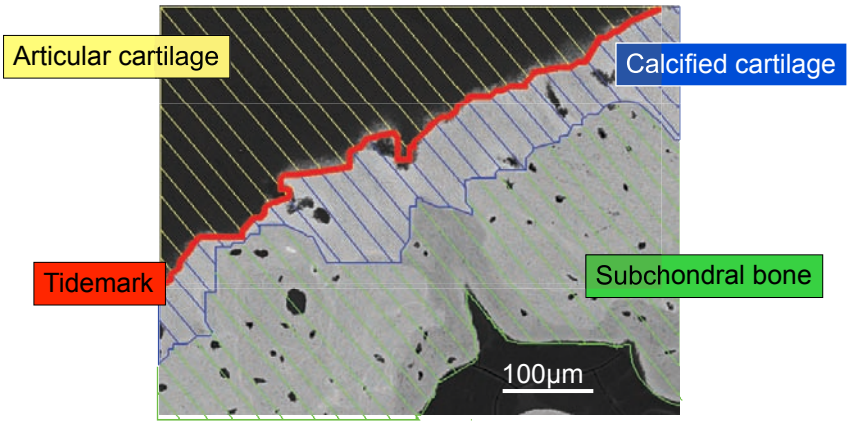

XRF-scans at HASYLAB-L

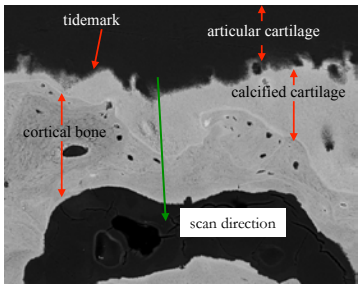

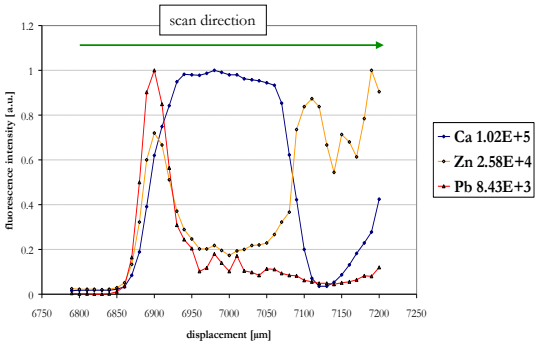

Patella - line scan

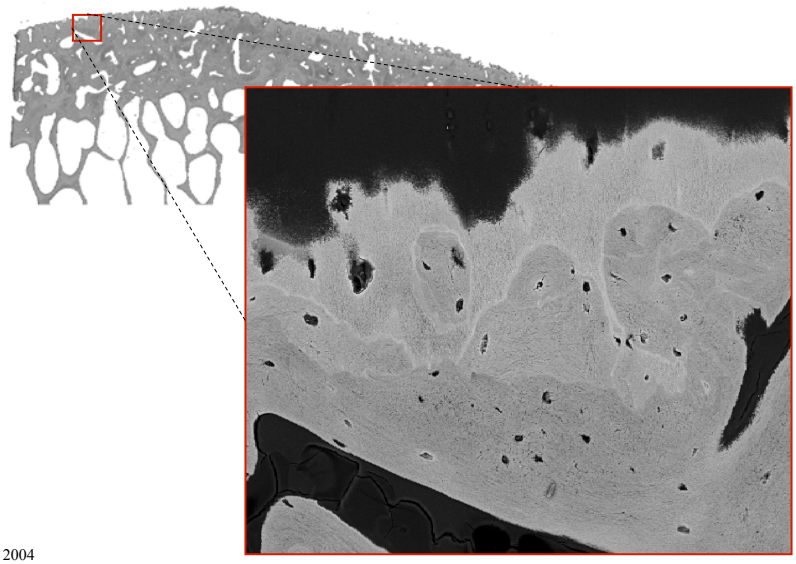

Interpretation: Sample Thickness Effect

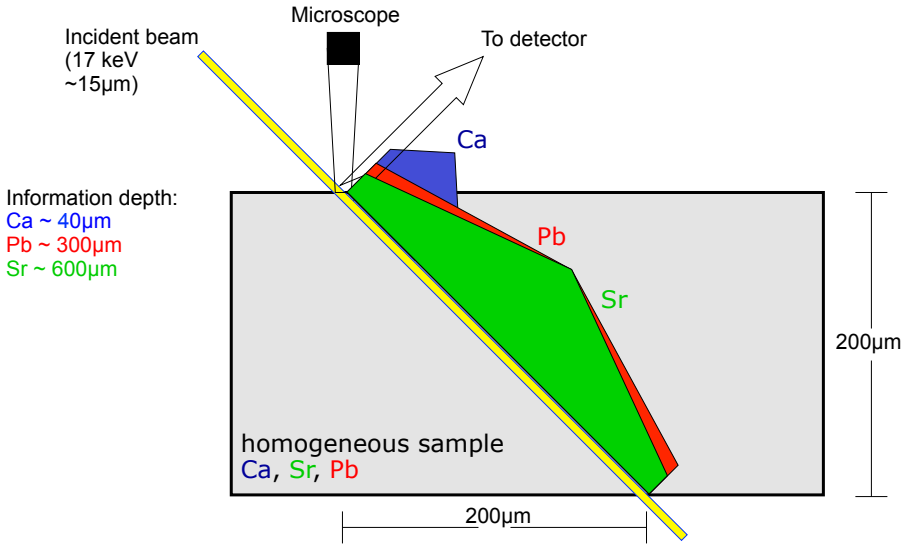

Interpretation: Sample Thickness Effect

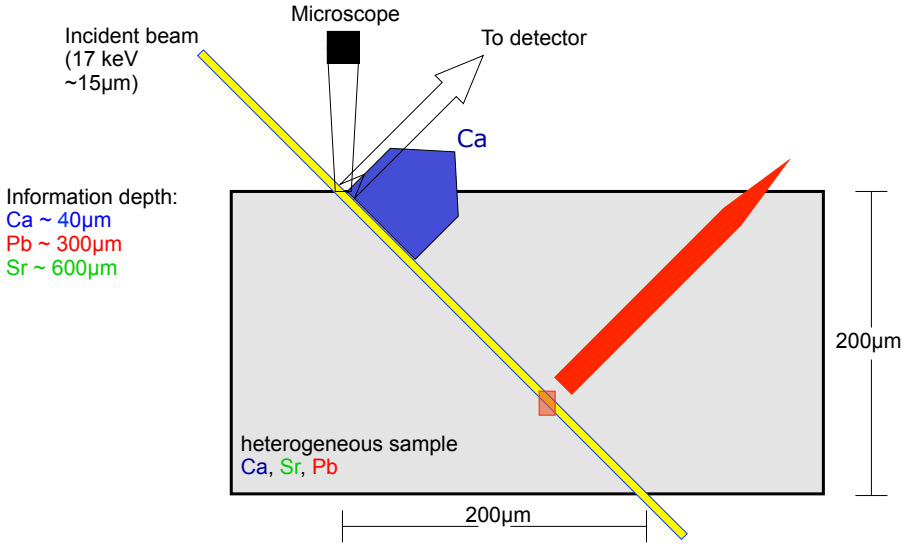

Confocal XRF

Setup at ANKA Fluo Beamline:

Focal size: ~10-20 µm
Depthresolution: ~15-20µm

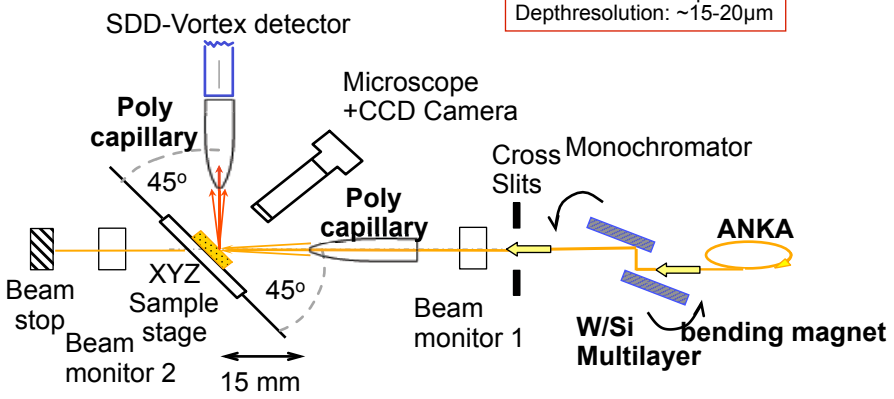

Confocal µ-XRF - Reason

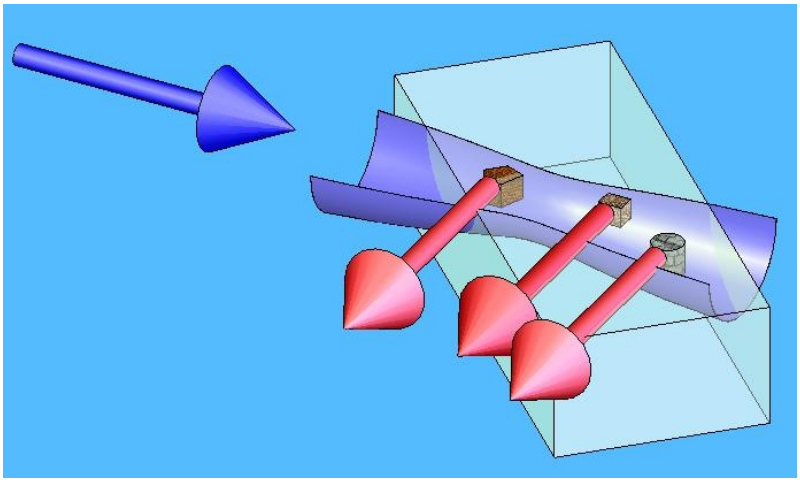

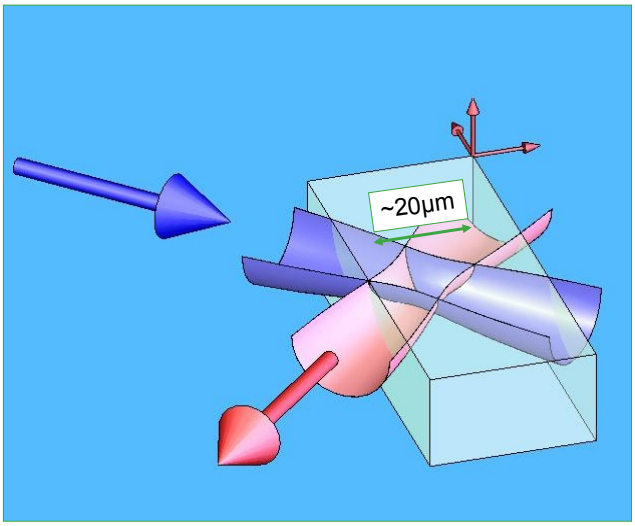
~20µm

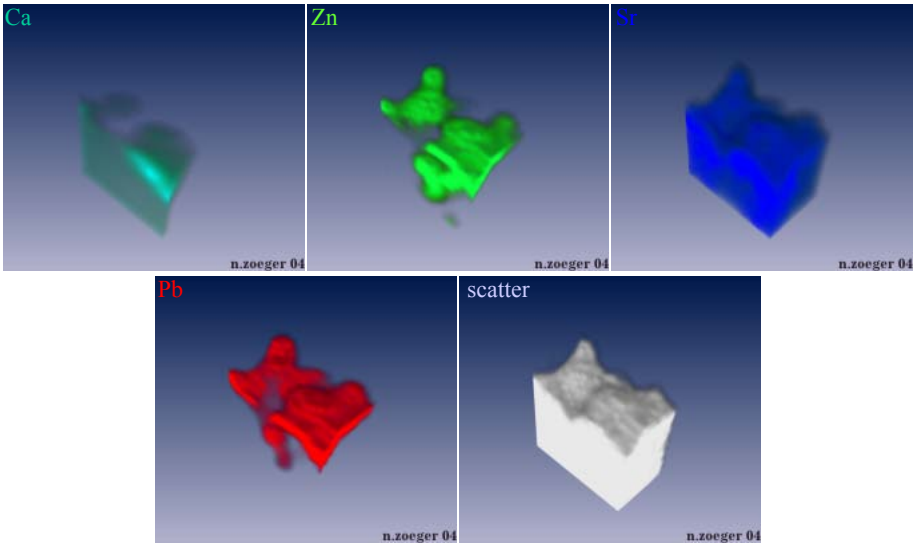
Ca
Zn
Sr
Pb
scatter
n.zoeger 04

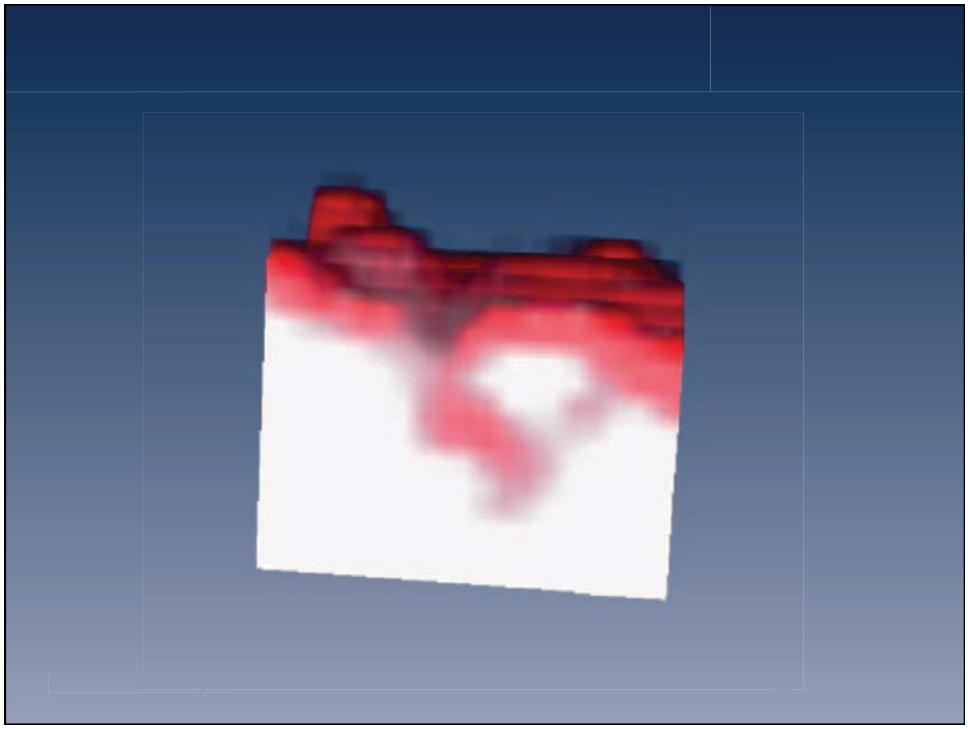

2D imaging :Element Maps

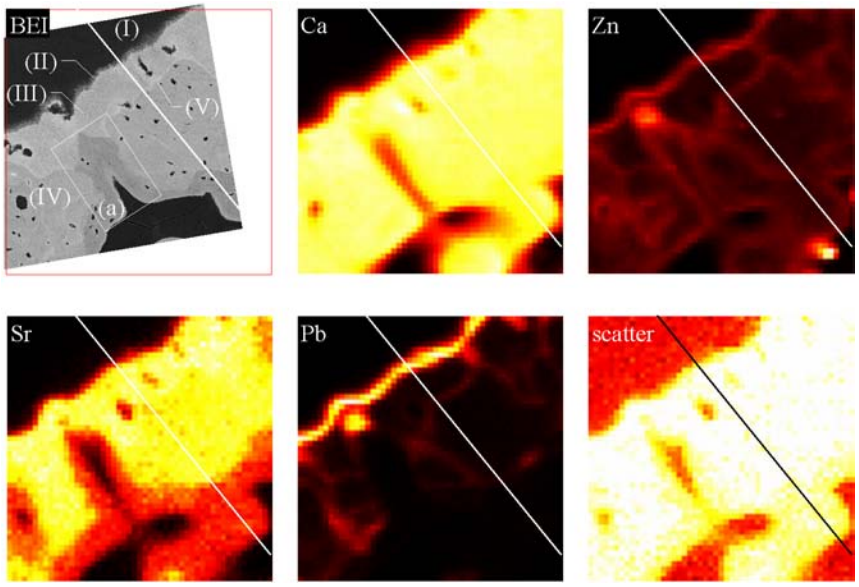

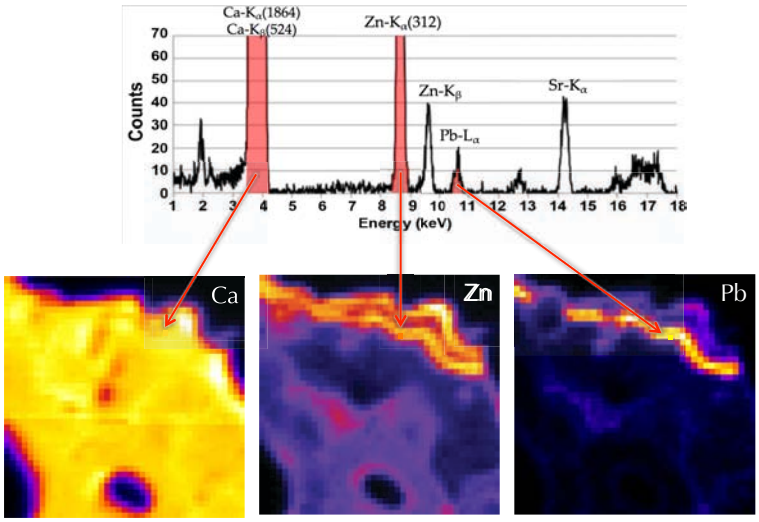

OsteoArthritis and Cartilage (2006) **14**, 906–913

doi:10.1016/j.joca.2006.03.001

Osteoarthritis and Cartilage

International Cartilage Repair Society

OARSI OSTEOARTHRITIS RESEARCH SOCIETY INTERNATIONAL

Lead accumulation in tidemark of articular cartilage

N. Zoeger Ph.D.†*, P. Roschger Ph.D.‡, J. G. Hofstaetter M.D.‡§, C. Jokubonis†, G. Pepponi Ph.D.‖, G. Falkenberg Ph.D.¶, P. Fratzl Ph.D.††, A. Berzlanovich M.D.‡‡§§, W. Osterode M.D., Ph.D.‖‖, C. Streli Ph.D.† and P. Wobrauschek Ph.D.†

† *Vienna University of Technology, Atominstitut, Stadionallee 2, 1020 Vienna, Austria*
‡ *Ludwig Boltzmann Institute of Osteology, Hanusch Hospital of WGKK and AUVA Trauma Centre Meidling, 4th Medical Department, Hanusch Hospital, Vienna, Austria*
§ *Department of Orthopaedics, Vienna General Hospital, Medical University of Vienna, A-1090 Vienna, Austria*
‖ *ITC-irst, Centro per la Ricerca Scientifica e Tecnologica, via Sommarive 18, 38050 Povo, Trento, Italy*
¶ *Hamburger Synchrotronstrahlungslabor HASYLAB am Deutschen Elektronen-Synchrotron, Notkestrasse 85, 22603 Hamburg, Germany*
†† *Max-Planck Institute of Colloids and Interfaces, Department of Biomaterials, Am Mühlenberg, D-14476 Potsdam-Golm, Germany*
‡‡ *Department of Forensic Medicine, Medical University of Vienna, A-1090 Vienna, Austria*
§§ *Department of Forensic Medicine, University of Munich, D-80377 Munich, Germany*
‖‖ *Universitätsklinik für Innere Medizin IV, Vienna General Hospital, Medical University of Vienna, A-1090 Vienna, Austria*

XANES of the Pb-LIII edge at the tidemark

Micro XANES @ ANKA, SUL-X

Samples:
Synthetic Hydroxyapatite Standard (400ppm)
Human Patella Sample

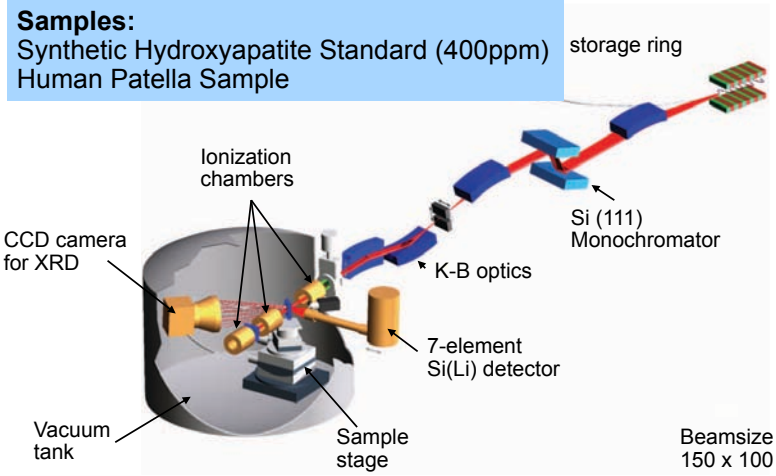

Beamsize at sample:
150 x 100 µm^2 (hor x ver)

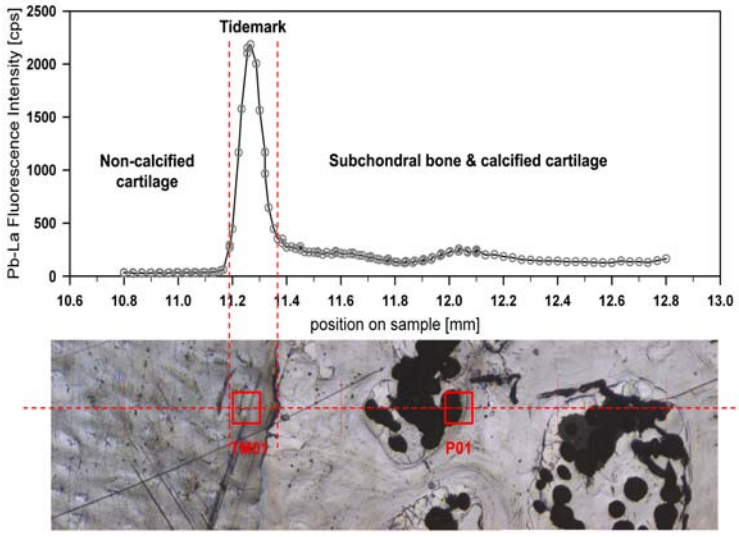

TECHNISCHE UNIVERSITÄT WIEN
Vienna University of Technology

Pb compounds

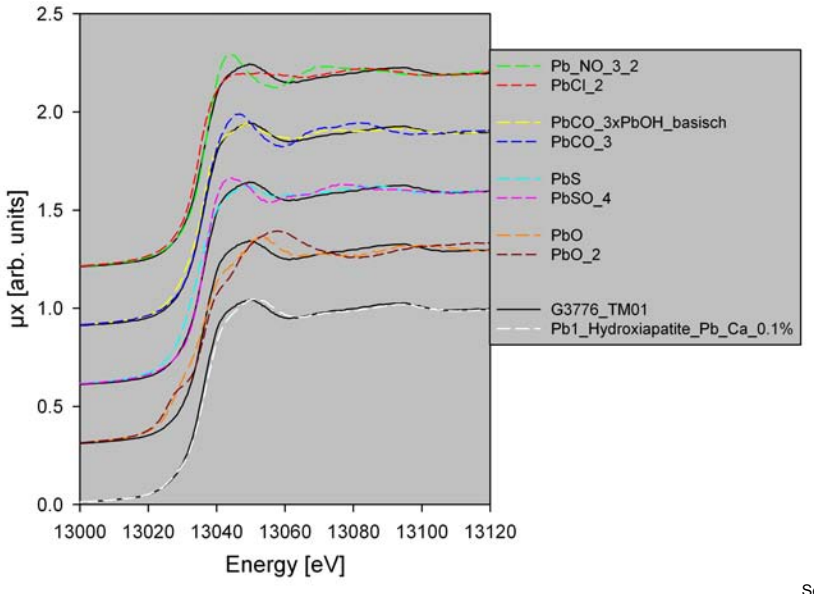

TECHNISCHE UNIVERSITÄT WIEN
Vienna University of Technology

Comparison with standards

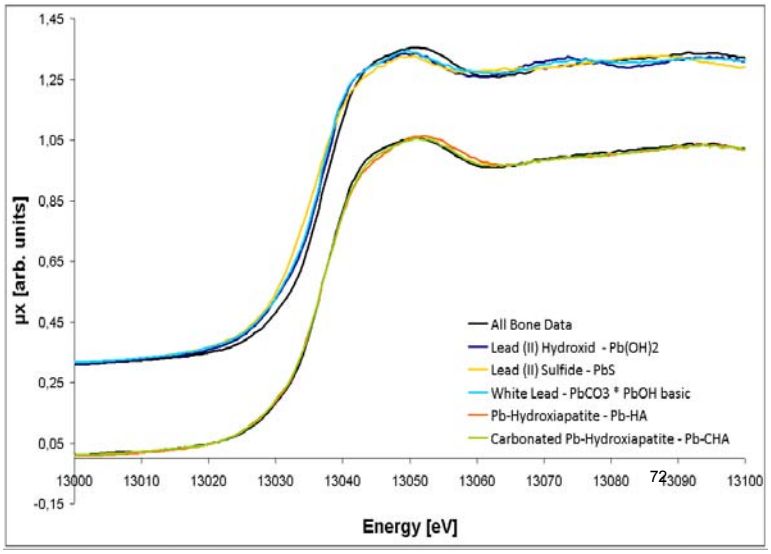

Pb-LIII XANES

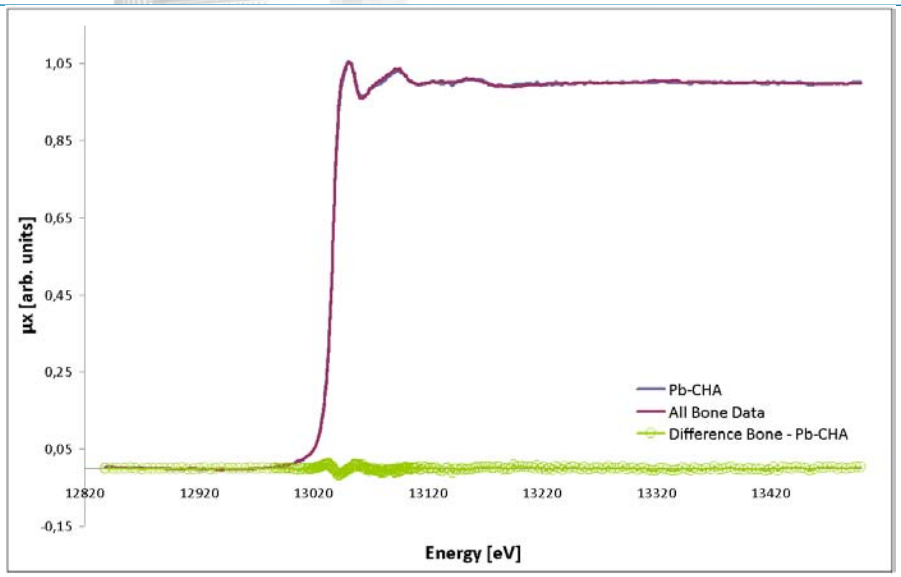

Comparison bone –Pb-CHA

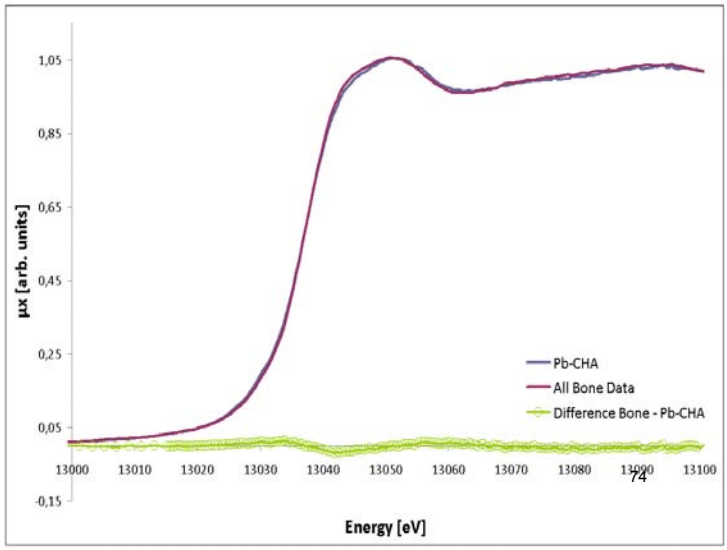

Pb-CHA fits to all bone data

TECHNISCHE UNIVERSITÄT WIEN
Vienna University of Technology

Comparison tidemark-trabecular bone

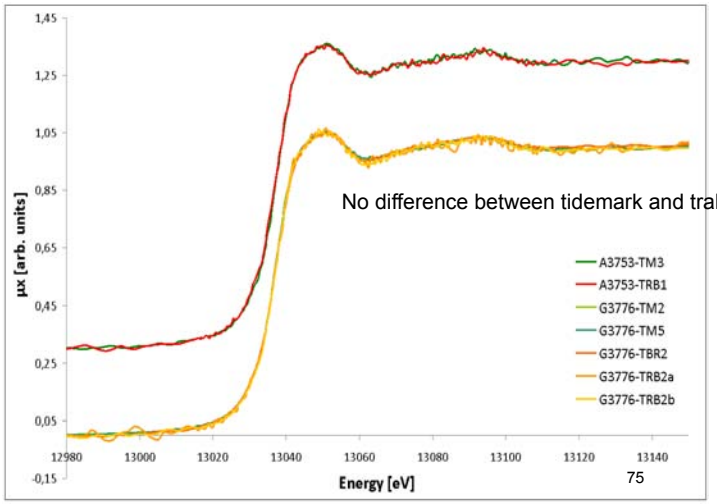

No difference between tidemark and trabecular bone

75

TECHNISCHE UNIVERSITÄT WIEN
Vienna University of Technology

ATOMINSTITUT

Journal of Synchrotron Radiation

Assessment of chemical species of lead accumulated in tidemarks of human articular cartilage by X-ray absorption near-edge structure analysis

Florian Meirer,[a,b] Bernhard Pemmer,[a]* Giancarlo Pepponi,[b] Norbert Zoeger,[c] Peter Wobrauschek,[a] Simone Sprio,[d] Anna Tampieri,[d] Joerg Goettlicher,[e] Ralph Steininger,[e] Stefan Mangold,[e] Paul Roschger,[f] Andrea Berzlanovich,[f] Jochen G. Hofstaetter[c,g] and Christina Streli[a]

[a]Atominstitut, Vienna University of Technology, 1020 Wien, Austria, [b]MNALab, CMM-Int, Fondazione Bruno Kessler, Via Sommarive 18, 38123 Trento, Italy, [c]Istituto di Scienza e Tecnologia dei Materiali Ceramici CNR, Faenza, Italy, [d]Institute for Synchrotron Radiation, Karlsruhe Institute of Technology, Campus South, 76344 Eggenstein-Leopoldshafen, Germany, [e]Ludwig Boltzmann Institute of Osteology, Hanusch Hospital of WGKK and AUVA Trauma Centre Meidling, 4th Medical Department, Hanusch Hospital, Vienna, Austria, [f]Department of Forensic Medicine, Medical University of Vienna, A-1090 Vienna, Austria, and [g]Department of Orthopaedics, Vienna General Hospital, Medical University of Vienna, A-1090 Vienna, Austria.
E-mail: bpemmer@ati.ac.at

A highly specific accumulation of the toxic element lead was recently measured in the transition zone between non-calcified and calcified normal human articular cartilage. This transition zone, the so-called 'tidemark', is considered to be an active calcification front of great clinical importance. However, little is known about the mechanisms of accumulation and the chemical form of Pb in calcified cartilage and bone. Using spatially resolved X-ray absorption near-edge structure analysis (μ-XANES) at the Pb L_{III}-edge, the chemical state of Pb in the osteochondral region was investigated. The feasibility of the μ-XANES set-up at the SUL-X beamline (ANKA synchrotron light source) was tested and confirmed by comparing XANES spectra of bulk Pb-reference compounds recorded at both the XAS and the SUL-X beamline at ANKA. The μ-XANES set-up was then used to investigate the tidemark region of human bone (two patella samples and one femoral head sample). The spectra recorded at the tidemark and at the trabecular bone were found to be highly correlated with the spectra of synthetic Pb-doped carbonated hydroxyapatite, suggesting that in both of these very different tissues Pb is incorporated into the hydroxyapatite structure.

Keywords: X-ray absorption spectroscopy; Pb L_{III}-edge XANES; human bone; tidemark; trabecular bone.

1. Introduction

Exposure to the toxic element lead is associated with chronic diseases of the nervous, hematopoietic, skeletal, renal and endocrine systems (Järup, 2003). Pb is predominantly stored in the human skeleton, where approximately 95% of the total body burden is present (Wittmers *et al.*, 1988). Bone is a composite material consisting of an organic component of the matrix, which is predominantly of type-I collagen molecules, which assemble in a regularly staggered manner to form fibrils of several hundred nanometres diameter. These collagen fibrils are impregnated with and surrounded by small nanocrystallite particles of carbonated apatite (Fratzl *et al.*, 2004).

The tibia and patella have been widely used in epidemiologic studies to determine bone Pb levels by *in vivo* *K*-line X-ray fluorescence (XRF). However, owing to the large information depth (~2 cm) when considering Pb *K*-lines (75 keV photons) in *in vivo* XRF analysis, signals are detected from a large bone volume and lack spatial resolution.

In recent studies we investigated the spatial distribution of Pb in the osteochondral region of normal human joints (Zoeger *et al.*, 2006, 2008) using Pb *La* fluorescence lines

Trace Element Distribution in Trabecular and Cortical bone of Fractured Femoral Necks of Postmenopausal Osteoporotic Women: A Synchrotron µ-XRF Imaging study

B. Pemmer[1], A. Roschger[1, 2], J. G. Hofstaetter[2, 3], P. Wobrauschek[1], R. Simon[4], P. Roschger[2], K. Klaushofer[2], C. Streli[1]

[1)] Atominstitut, Technische Universitaet Wien, Stationallee 2, 1020 Vienna, Austria
[2)] Ludwig Boltzmann Institute of Osteology at the Hanusch Hospital of WGKK and AUVA Trauma Centre Meidling, 1st Med. Dept., Hanusch Hospital, Vienna, Austria
[3)] Department of Orthopaedic Surgery, Vienna General Hospital, Medical Univ. of Vienna, Austria
[4)] Karlsruhe Institute of Technology, Institute for Synchrotron Radiation, Hermann-von-Helmholtz-Platz 1, D-76344 Eggenstein-Leopoldshafen, Germany

Elemental Distribution in (Osteoporotioc) Bone

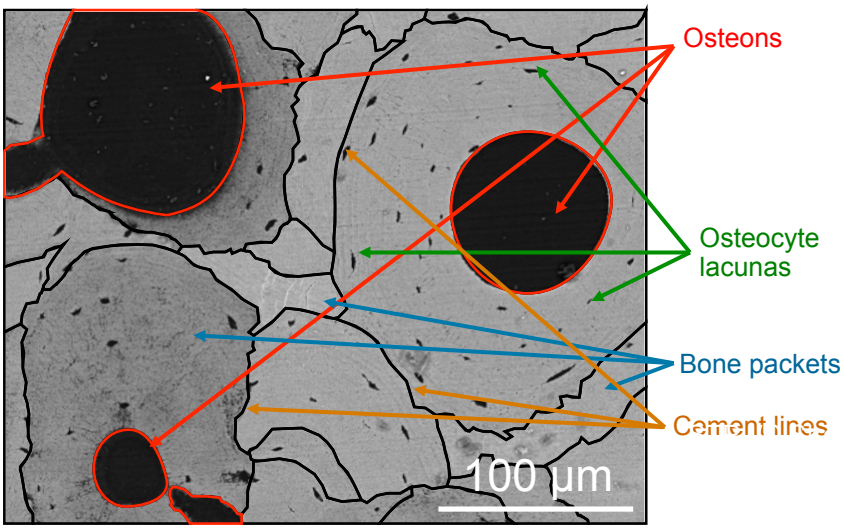

Elemental Distribution in (Osteoporotioc) Bone

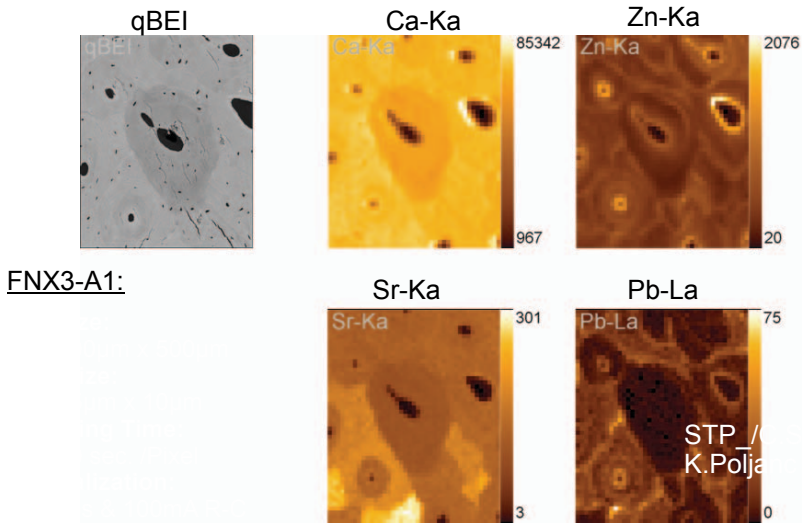

Elemental Distribution in (Osteoporotioc) Bone

Bone Packets vs. Cement lines - Lead:

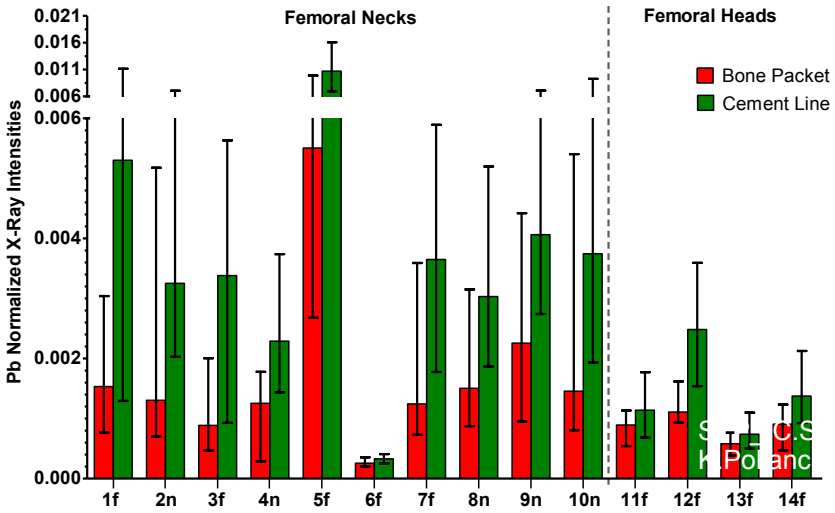

Pb levels sign. increased in cement lines

Bone Packets vs. Cement lines - Zinc:

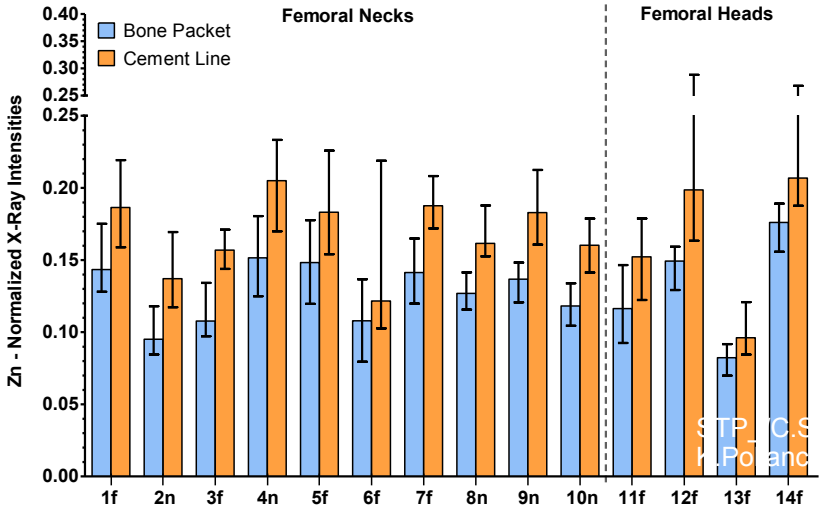

Zn levels sign. increased in cement lines

Summary / Conclusions:

- Distinct localization of zinc & lead
  - compact bone & trabecular bone
- Accumulation in cement lines:
  - Zinc & Lead
- Osteoporotic fractured vs. controls:
  - no significant differences in element distribution
- Differences between sample groups - FNX vs. HHX:
  - no significant differences in zinc distribution
  - Less calcium, lead and strontium in HHX samples

B. Pemmer, A. Roschger, A. Wastl, J. G. Hofstaetter, P. Wobrauschek, R. Simon, H. W. Thaler, P. Roschger, K. Klaushofer, and C. Streli, "Spatial distribution of the trace elements zinc, strontium and lead in human bone tissue.," Bone, vol. 57, no. 1, pp. 184–93, Nov. 2013.